Tetrahedron: *Asymmetry* 20 (2009) 2247–2256

Contents lists available at ScienceDirect

Tetrahedron: *Asymmetry*

journal homepage: www.elsevier.com/locate/tetasy

Enantioselective synthesis, chiroptical properties and absolute configuration of 3-aminosubstituted isothiazole S-oxides

Alessandro Casoni [a], Giuseppe Celentano [a], Francesca Clerici [a,*], Alessandro Contini [a], Maria Luisa Gelmi [a], Giuseppe Mazzeo [b], Sara Pellegrino [a], Carlo Rosini [b]

[a] *DISMAB, Sezione di Chimica Organica 'A. Marchesini', Università di Milano, Via Venezian 21, 20133 Milano, Italy*
[b] *Dipartimento di Chimica, Università della Basilicata, via N. Sauro 85, 85100 Potenza, Italy*

ARTICLE INFO

Article history:
Received 27 July 2009
Accepted 20 August 2009
Available online 15 September 2009

ABSTRACT

Herein we report a mild and efficient method to synthesize chiral 3-aminosubstituted isothiazole sulfoxides taking advantage of (+)- and (−)-((8,8-dichlorocamphoryl)sulfonyl)oxaziridine under microwave irradiation. The determination of the absolute configuration of the chiral sulfoxide was achieved by theoretical calculation of the CD spectra. The reason for the observed stereoselectivity was enlightened by means of analysis of our data using DFT calculations.

1. Introduction

The importance of the isothiazole nucleus containing compounds appears to have grown over the recent years. New synthetic approaches and unprecedented reactions have been reported and numerous technical and pharmaceutical applications have been discovered.[1a–e]

In particular, both the synthesis and the chemical reactivity of 3-aminoisothiazole 1,1-dioxides have been studied by us for many years, and the important transformations and applications of these compounds have been found as precursors both to N- and/or S-containing heterocycles and to open chain compounds through ring-opening reactions.[2] Moreover, it has to be remembered that several representatives of the 3-aminoisothiazole dioxide series display interesting biological activity as antiproliferating agents.[3–5] Very recently we described a mild and efficient method to synthesize chiral racemic 3-aminosubstituted isothiazole sulfoxides by taking advantage of arylsulfonyloxaziridines.[6] It should be taken into account that the preparation of chiral compounds has been an important and challenging area of contemporary synthetic organic chemistry, and that especially the preparation of new chiral ligands for application in asymmetric catalysis continues to occupy the research focus these days. New classes of ligands that might offer new opportunities for applications or provide insight into the fundamental chemical processes are always interesting. One relatively rare class of ligands is that in which the stereogenicity resides not at carbon atoms, but at heteroatomic sites such as sulfur atoms.[7] This phenomenon prompted us to study the asymmetric oxidation of the prochiral sulfur to produce enantiopure 3-aminoisothiazole derivatives (Scheme 1). Computational analysis of the oxidation mechanism was performed for a better understanding of the observed enantioselectivity.

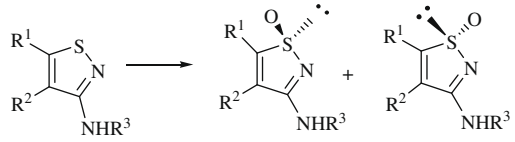

1 (*R*)-**2** (*S*)-**2**

Scheme 1. 3-Aminosubstituted-isothiazoles **1** and S-oxides (*R*)-**2** and (*S*)-**2**.

Moreover, a study of the possibility to assign the absolute configuration of the new 3-aminosubstituted isothiazole S-oxides by applying methods based on the quantum chemical calculation of the chiroptical properties has also been performed.

2. Results and discussion

2.1. Asymmetric oxidation

With the aim of synthesizing optically active sulfoxides, we considered either the enantioselective oxidation using chiral oxidizing reagents or the diastereoselective approach where the introduction of a stereogenic centre on the starting isothiazole would be potentially capable of providing asymmetric induction.

2.1.1. Diastereoselective oxidation

This basic process makes use of the proximity of a defined stereogenic centre to relay stereochemistry to the newly formed sulfoxide. The 3-(*S*)-(1-phenylethyl)aminoisothiazole **1a** was prepared starting from enantiomerically pure (*S*)-1-phenylethylamide **2** by a known protocol through the intermediate isothiazolone **3** (Scheme 2).[8]

* Corresponding author. Tel.: +39 0250314472; fax: +39 0250314476.
E-mail address: francesca.clerici@unimi.it (F. Clerici).

0957-4166/$ - see front matter © 2009 Elsevier Ltd. All rights reserved.
doi:10.1016/j.tetasy.2009.08.023

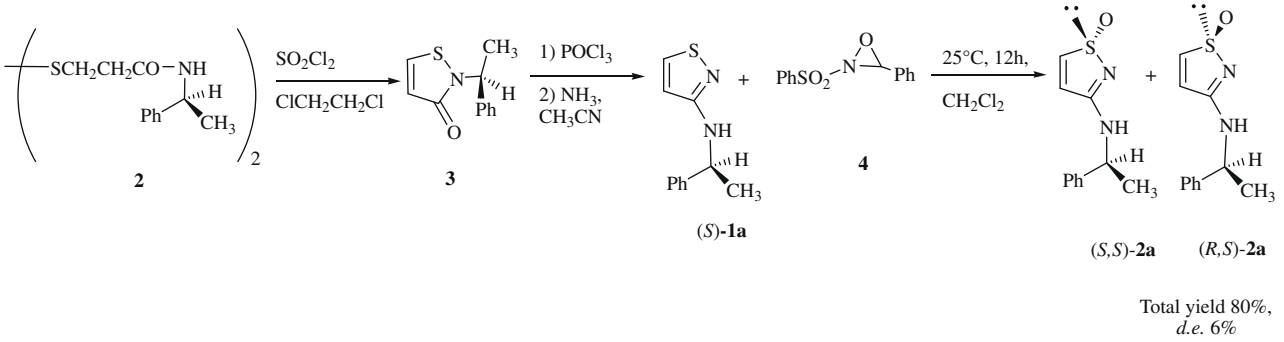

Scheme 2. Synthesis and oxidation of 3-(*S*)-(1-phenylethyl)aminoisothiazole **1a** to (*S,S*)-**2a** and (*R,S*)-**2a**.

In a previously reported study we have shown that arylsulfonyloxaziridines were able to selectively oxidize 3-aminosubstituted isothiazoles to the chiral racemic corresponding sulfoxides in a mild and efficient way.[6] We applied such a method to (*S*)-**1a** by using *N*-phenylsulfonyl-4-phenyl-oxaziridine **4** as the oxidant but, in spite of the good yields, the reaction, unfortunately, gave very low diastereoselection (de 6%). This unsatisfactory result could be explained by arguing that the chiral amino group is too far from the prochiral sulfur atom to exert a powerful influence on the stereochemical outcome of the oxidation.

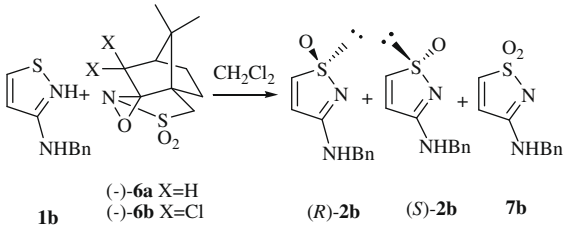

Scheme 3. Oxidation of 3-alkylaminoisothiazoles **1b** with oxaziridines (−)-**6a**,**b**.

2.1.2. Enantioselective oxidation

Enantiopure *N*-sulfonyloxaziridines which are known to be useful reagents for the enantioselective oxidation of a variety of substrates in high and predictable stereoselectivity were considered.[9] Among the different types of the available enantiopure oxaziridines, compounds **5** and **6a**,**b**,**c**,**d** were evaluated (Fig. 1).[10,11]

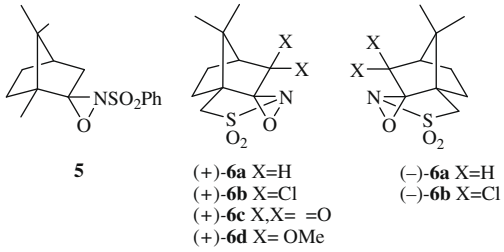

Figure 1. Structures of enantiopure *N*-sulfonyloxaziridines **5**, **6**.

For the first experiments we chose *N*-benzylaminoisothiazole **1b** which was reacted with *N*-sulfonyloxaziridines **5**, (+)-**6c** and (+)-**6d**, but the desired isothiazole sulfoxide **2b** was not obtained in appreciable yields or in good chemoselectivity either at room or higher temperature, or by irradiation with microwaves or sonication. Improved results were obtained with *N*-sulfonyloxaziridines (−)-**6a** and (−)-**6b**, which oxidized 3-aminoisothiazole **1b** at room temperature in CH_2Cl_2, producing a mixture of enantiomers (*R*)-**2b** and (*S*)-**2b** in appreciable yields (60–62%) and with reasonable chemoselectivity (**7b**: 15–20%) but over a very long reaction time (168–240 h) (Scheme 3). Despite the good yields and selectivity for the sulfo format, disappointing results were obtained in terms of enantioselectivity with both (−)-**6a** (ee 10%) and (−)-**6b** (ee 18%) (Table 1, entries 1 and 2). In both cases, one enantiomer, the (*R*)-enantiomer, was formed in slight excess as shown by chiral HPLC analyses. The absolute configuration was established as described later.

Comparable results were obtained by performing the reaction with (+)-**6b**, which afforded a mixture of (*R*)-**2b** and (*S*)-**2b** (Table 1, entry 3). As expected, chiral HPLC analysis revealed that the major enantiomer was the counterpart of the one obtained with (−)-**6b**, that is, the (*S*)-isomer. The best results in terms of yields and selectivity were obtained by performing the reaction under microwave irradiation. When a solution of **1b** and (−)-**6b** (1 equiv) in CH_2Cl_2 was irradiated at 400 W (80 °C) enantiomers (*R*)-**2b** and (*S*)-**2b** were produced in 82% overall yield and 50 ee%, together with small amounts of **7b** (8%) (Table 1, entry 5).

Table 1
Oxidation of **1b** with (−)- and (+)-**6a**,**b**

Entry	Oxidant	React. cond.[a]	Time (h)	Yield % **7**	ee %
1	(−)-**6a**	**A**	240	62 (20)	10
2	(−)-**6b**	**A**	168	60 (18)	18
3	(+)-**6b**	**A**	168	60 (15)	20
4	(−)-**6a**	**B**	7	24 (10)	24
5	(−)-**6b**	**B**	1	82 (8)	50
6	(+)-**6b**	**B**	1	80 (7)	55

[a] Reaction conditions: **A**: CH_2Cl_2, 25 °C; **B**: μW, 400 W, 80 °C.

As expected, comparable results were obtained with (+)-**6b** (Table 1, entry 6). It was evident that microwave irradiation enhanced the rate of the reaction (1 h vs 168 h) and the enantioselectivity (50% vs 20%). The reaction rate was higher with (−)-**6b** (Table 1, entry 5), as compared to (−)-**6a** (Table 1, entry 4) and this is consistent with the fact that electronegative groups attached to the oxaziridine carbon in *N*-sulfonyloxaziridines increase the rate of the oxidation.[12]

Comparable results were obtained with **1c** (Scheme 4, Table 2, entries 1 and 2).

Finally, the oxidation of (*S*)-**1a** with (+)- and (−)-**6b** showed similar behaviour and a mixture of 3-(*S*)-(1-phenylethyl)aminoisothiazole-(*S*)-1-oxide (*S,S*)-**2a** and 3-(*S*)-(1-phenylethyl)aminoisothiazole-(*R*)-1-oxide (*S,R*)-**2a** was formed over a very long reaction time (240 h) and in unsatisfactory yields (36%) and only 8% de (Scheme 4, Table 2, entry 3). However, considerable improvements in yields (50%) and diastereoselectivity (60%) were obtained by performing the reaction under microwave irradiation (400 W), with an equimolar amount of (+)-**6b** in CH_2Cl_2 at 80 °C (Table 2, entry 4). As expected, analogous results in terms of yield and de% were

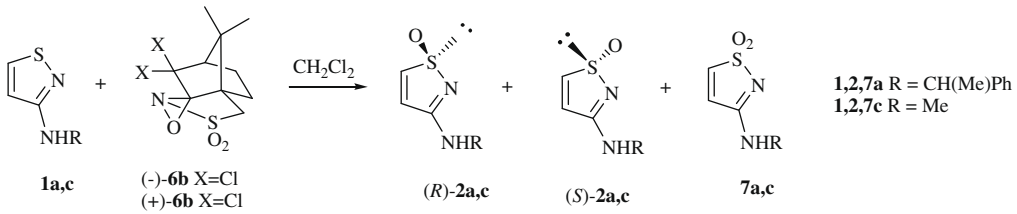

Scheme 4. Oxidation of 3-alkylaminoisothiazoles **1a**,**c** with oxaziridines (−)- and (+)-**6b**.

Table 2
Oxidation of 3-alkylaminoisothiazoles **1c**,**a** with oxaziridines (−) or (**+**)-**6b**

Entry	Compd	R	Oxidant	React. cond.[a]	Time (h)	Yield % **7**	ee %
1	**1c**	Me	(−)-**6b**	**B**	2.3	70 (15)	43.6
2	**1c**	Me	(+)-**6b**	**B**	2.5	60 (10)	49.6
3	**1a**	CH(Me)Ph	(+)-**6b**	**A**	240	36 (10)	8[b]
4	**1a**	CH(Me)Ph	(+)-**6b**	**B**	2.5	50 (14)	60[b]
5	**1a**	CH(Me)Ph	(−)-**6b**	**B**	3	56 (16)	40[b]

[a] Reaction conditions: **A**: CH_2Cl_2, 25 °C; **B**: μW, 400 W, 80 °C.
[b] Diastereoisomeric excess.

obtained by performing the reaction with (−)-**6b**, which afforded the opposite ratio of enantiomers **2a** (Table 2, entry 5).

The presence of the stereocentre on the isothiazole **1a** did not seem to significantly influence the formation of the new stereocentre on the sulfur atom. With this procedure, we were able to isolate the diastereoisomeric compounds (*S*,*S*)-**2a** and (*R*,*S*)-**2a** in pure form (98% purity, chiral HPLC analyses) after column chromatography and crystallization with H_2O/MeOH.

Theoretical and experimental studies support an S_N2 type reaction for the oxygen transfer from *N*-sulfonyloxaziridines to the sulfur nucleophiles. It was concluded that molecular recognition was largely steric in origin as dictated by the substituents on both the oxaziridines and substrates.[13–15] Apparently, the sulfur atom on the planar isothiazole system of compounds **1a**, **1b** and **1c**, is not surrounded by a sterically demanding group. Accordingly, we prepared isothiazole derivatives **1d**–**g** substituted at C-4 or C-5 with a halogen, aiming to evaluate the role of the substituent in the selectivity of the process.

The new compounds, 3-benzylamino-4-chloro-isothiazole **1d** and 3-benzylamino-4-bromo-isothiazole **1e** were synthesized by a known procedure with some modifications (Scheme 5).[16–18]

To synthesize the previously unreported compound **1f** bearing a bromine atom on C-5, we generated the 5-lithium anion by reacting **1b** with LDA at −60 °C, and capturing the anion with BrCN to afford the desired compound **1f** (Scheme 6).[19,20]

The sulfoxidation of compounds **1d**–**g** was performed by applying the optimum reaction conditions described above (i.e., μW, 400 W, 80 °C) using both (+)-**6b** and (−)-**6b** as the oxidants (Scheme 7). The results are reported in Table 3. The 5-chloro derivative **1g** afforded the corresponding sulfoxides **2g** in very good overall yields (83%, 12 h) but with very low enantiomeric excess (Table 3, entry 1).

Similar results were obtained with **1f**, in which the bromine substituent resides at C-5 (Table 3, entry 2). However, when the

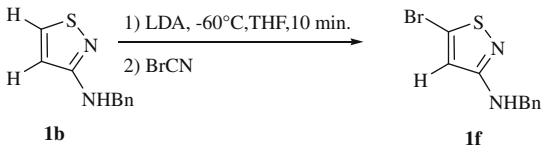

Scheme 6. Synthesis of compound **1f**.

reaction was performed on **1e**, with a bromine atom on C-4, we observed the formation of **2e** in very good overall yield (80%) and satisfactory reaction time (12 h) with a marked enantiomeric excess (65%) (Table 3, entry 4). An increase in the ee% (65%) was also observed with the 4-chloro derivative **1d** (Table 3, entry 2). In this last case, a longer reaction time was required. It was apparent that the presence of a halogen atom on C-5 had no influence on the enantioselectivity of the oxidation reaction but the presence of a halogen atom on C-4 significantly increased the formation of one enantiomer with respect to the other. The observed enantioselectivity for the oxidation reactions was rationalized by performing DFT calculations in order to analyze the transition structures leading to (*R*)- and (*S*)-enantiomers.

2.2. Configuration assignment

As stated previously, compounds (*S*,*S*)-**2a** and (*R*,*S*)-**2a** were obtained in crystal form. Unfortunately, many attempts to grow crystals suitable for X-ray analysis in order to define the absolute configuration of the sulfur in the sulfoxide group, failed. In order to solve this problem, we decided to make use of chiroptical spectroscopy. In order to determine the absolute configuration of the new 3-aminosubstituted isothiazole S-oxides, we decided to apply the methods based on the quantum chemical calculation of the optical rotation, obtained for an arbitrarily assumed absolute con-

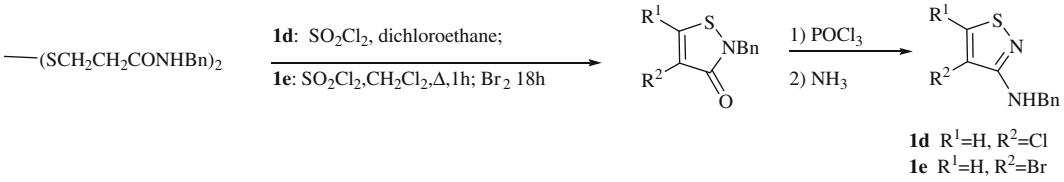

Scheme 5. Synthetic strategy for compounds **1d**,**e**.

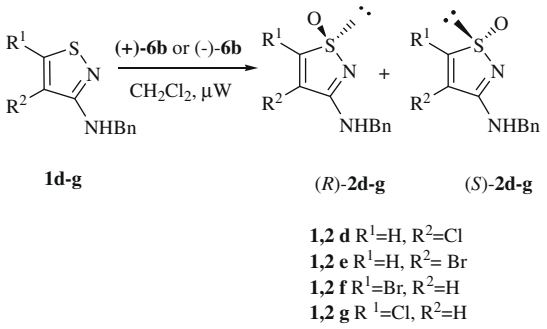

Scheme 7. Oxidation of 4- or 5-substituted 3-benzylaminoisothiazoles with oxaziridines (+)-**6b** or (−)-**6b**.

Table 3
Oxaziridine oxidation of isothiazoles **1d–g**

Entry	Compd	R^1	R^2	Oxaziridine[a]	Time (h)	Yield %	ee %
1	**1g**	Cl	H	(+)-**6b**	12	83	6
2	**1f**	Br	H	(+)-**6b**	12	70	6.4
3	**1d**	H	Cl	(+)-**6b**	24	54	65
4	**1e**	H	Br	(+)-**6b**	12	80	65

[a] Compound (−)-**6b** was also tested affording comparable results in terms of yields and ee, obviously in favour of the opposite enantiomer.

figuration and the comparison with the experimental data. This method was introduced in 1997[21a,b,22a,b] however since then, several papers appeared in this field: accounts of these investigations can be found in Refs. 21c and 23, whilst in Ref. 24 number of applications to the determination of absolute configurations of new molecules can be found. Clearly this approach requires that the simulated values are fully reliable in sign and order of magnitude. Since the 1997 papers cited above, where the first optical rotation calculations were carried out using the Hartree–Fock/small basis set approach, many studies have been carried out at different levels of theory to set up methods which couple reliability and accuracy to a reasonable computational effort.[23] From this point of view the investigations of Stephens et al. have demonstrated that Time Dependent Density Functional Theory (TDDFT) calculations with the B3LYP hybrid functional and extended basis sets (i.e., aug-cc-pVDZ or higher) give completely reliable results (with an acceptable computational effort) in reproducing experimental optical rotations of at least 100 deg $[dm\ g/cm^3]^{-1}$.[25] Hence we decided to apply the Stephens protocol to assign the absolute configuration of these new compounds by predicting their optical rotations and comparing these data with the experimental values. The necessary experimental data were taken from 3-methylaminoisothiazole 1-oxide, that is, a compound having a small size (this fact allows to use the extended aug-cc-pVDZ basis set, suggested by Stephens, even on a common desktop PC) and a reduced conformational freedom, only due to the possible rotations around the C(3)–N bond: for these reasons a heavy computational effort can be excluded. Then, 3-methylaminoisothiazole **1c** was oxidized by (−)- and (+)-**6b** by obtaining the corresponding sulfoxide **2c** with $[\alpha]_D = -60$ (*c* 1, methanol), ee 43.6% and +69 (*c* 1, methanol), ee 49.6%. From these numbers we can deduce an absolute value for $[\alpha]_D$ of 3-methylaminoisothiazole 1-oxide of 138 in methanol. Changing the solvent from methanol to either ethanol or chloroform causes some variations in the absolute value, but, most importantly, no changes of sign are observed: it becomes +165 (*c* 1, ethanol) and +225 (*c* 1, chloroform). In addition, the electronic circular dichroism (ECD) spectrum has also been measured in ethanol and it is reported, together with the absorption spectrum in Figure 2.

The electronic spectrum shows two main regions of absorption: a low energy one centred at about 330 nm (ε_{max} 4000 ca.) and extending from 380 to 280 nm, and a high energy one which increases monotonically from 280 nm down to 200 nm, where an ε value of about 15,000 can be measured. In the ECD spectrum a very

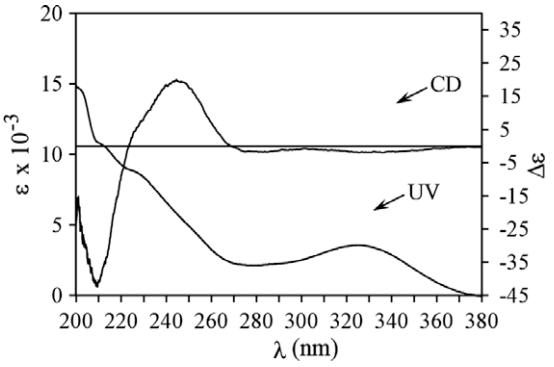

Figure 2. Absorption (UV curve) and circular dichroism (CD curve) of (+)-3-methylaminoisothiazole 1-oxide **2c** in ethanol.

broad, negative Cotton effect can be observed between 380 and 280 nm ($\Delta\varepsilon_{max}$ of the order of −1), followed by a strong ($\Delta\varepsilon$ +20) positive CD band centred at 250 nm, in turn followed by a third Cotton effect at 210 nm with $\Delta\varepsilon$ −42. We can now attempt at reproducing the above-mentioned chiroptical data by means of some TDDFT/B3LYP/aug-cc-pVDZ calculations. The calculations object of this investigation have been carried out as described in Section 4.1. Assuming an (*S*)-absolute configuration for the sulfur stereogenic centre of 3-methylaminoisothiazole 1-oxide **2c**, by means of a sequence of molecular mechanics/DFT calculations two different conformers have been found in the gas phase, the structure, relative energy and population of which are reported in Figure 3.

The most stable conformer (conf. 1) is characterized by having the methyl group linked to the nitrogen atom on the same side of the N(2), when the same group is placed near to the vinyl hydrogen linked to C(4) (conf. 2) the free energy increases significantly (+2.07 kcal/mol) leading to populations of 97% and 3%, respectively. The optical rotation prediction (TDDFT/B3LYP/aug-cc-pVDZ level of theory) gives +71 (conf. 1) and −119 (conf. 2): these values afford a weighted average value of +65. This figure, obtained for the (*S*)-configured compound, is of the same sign of the experimental number, even if, from a quantitative point of view, this number is, at maximum, almost 50% of the experimental value. In order to have a better agreement between experimental and predicted values we introduced the solvent effect, by means of the PCM model both in the optimization of the molecular geometry and in the calculation of the optical rotation.[26] The results are collected in Table 4 (ethanol), Table 5 (methanol) and Table 6 (chloroform).

Looking at Tables 4–6, it can be observed that: (i) conformer 1 remains, in all solvents, the most stable, and its population further increases in all of them; (ii) whilst in the gas phase we saw that the optical rotation of the most stable conformer was smaller in absolute value than the optical rotation of the second conformer, the situation is completely reversed in all the solvents; (iii) as a consequence, the theoretical rotation is determined, in practice, by the most stable conformer, even if the rotations of the two conformers are opposite in sign; (iv) the weighted average optical rotation (i.e., the number to be compared with the experimental value) is always positive for the (*S*)-absolute configuration, as observed experimentally for the three solvents: this strongly indicates the correlation (+)/(*S*) for 3-methylaminoisothiazole 1-oxide; (v) from a numerical

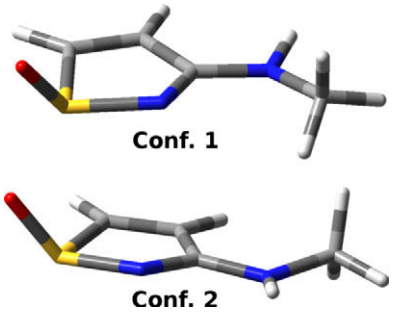

Figure 3. Stable conformers of (*S*)-3-methylaminoisothiazole 1-oxide **2c**.

Table 4
Relative-free energies with respect to the most stable conformer (kcal mol^{-1}), populations, $[\alpha]_D$ values (deg [dm g/cm^3]$^{-1}$) obtained at TDDFT/B3LYP/aug-cc-pVDZ level for each conformer of (*S*)-methylaminoisothiazole 1-oxide in ethanol

	ΔG	% Pop	Optical rotation	
			Calcd	Scaled
Conf. 1	0	99	+280	+277
Conf. 2	2.7	1	−76	−0.8
Total			276	

Table 5
Relative-free energies with respect to the most stable conformer (kcal mol^{-1}), populations, $[\alpha]_D$ values (deg [dm g/cm^3]$^{-1}$) obtained at TDDFT/B3LYP/aug-cc-pVDZ level for each conformer of (*S*)-methylaminoisothiazole 1-oxide in methanol

	ΔG	% Pop	Optical rotation	
			Calcd	Scaled
Conf. 1	0	99	+290	+287
Conf. 2	2.7	1	−74	−0.7
Total			286	

Table 6
Relative-free energies with respect to the most stable conformer (kcal mol^{-1}), populations, $[\alpha]_D$ values (deg [dm g/cm^3]$^{-1}$) obtained at TDDFT/B3LYP/aug-cc-pVDZ level for each conformer of (*S*)-methylaminoisothiazole 1-oxide in chloroform

	ΔG	% Pop	Optical rotation	
			Calcd	Scaled
Conf. 1	0	98	+213	+209
Conf. 2	2.25	2	−83	−1.7
Total			207	

point of view, it can be observed that the theory predicts similar values in ethanol and methanol (276 and 286, respectively) whilst the experimental figures are smaller (165 and 138, respectively). In other words, it seems that the present solvation model overestimates the effect of the alcoholic solvents and cannot reproduce the experimental difference between the experimental values in ethanol and methanol; (vi) by contrast, the agreement in chloroform results is excellent. To conclude this part, we can state that even if the PCM solvation model does not afford a fully quantitative agreement with the experiment, it reproduces the measured optical rotations in sign and order of magnitude and that the absolute configuration of (+)-3-methylaminoisothiazole 1-oxide **2c** is (*S*). We decided to try to further support the above-mentioned correlation by means of the TDDFT/B3LYP/aug-cc-pVDZ calculation of the ECD spectrum of this compound in the range 380–200 nm, in both the gas phase and ethanol.

In Figure 4 the predicted ECD spectra of (*S*)-3-methylaminoisothiazole 1-oxide as obtained as a weighted average of the ECD spectra of the two conformers, taking into account the first 30 excited states in both the gas phase and ethanol, are reported. The ECD spectra have been calculated in both the length and velocity formalism, these calculated spectra are almost coincident indicating the high level of the calculation. For this reason in Figure 4 only the velocity-form predicted spectra are reported. As far as the gas phase calculations are concerned, the positions of ECD intensity maxima in the theoretical spectrum do not perfectly match those of the theoretical spectrum (the predicted spectrum is considerably red shifted with respect to the experimental one, an effect of this type has been already observed in TDDFT calculations[27]) and the predicted ECD intensities are in general smaller than the experimental data. Nevertheless, the experimental spectrum shows a sequence of negative, positive, negative Cotton effects. The same features are reproduced in the theoretical spectrum, again confirming the (+)/(*S*) correlation found with the optical rotation calculations. Including the solvent (ethanol) effect in the above-mentioned calculation significantly improves the agreement between the calculated and experimental data, strongly supporting the (+)/(*S*) configurational correlation. In fact, the complete sequence of negative, positive and negative Cotton effects observed in the experimental spectrum is very well reproduced by the present calculations. In particular, a significant solvent effect can be observed in the intensities of the ECD bands, which are now very well simulated. It can also be seen that there is a reduction in the amount of red-shift of the predicted ECD bands with respect to the experimental ones. However, the remaining red-shift and the increase in intensity of the ECD bands could be responsible for the overestimation of the optical rotation data. We can now conclude that (+)-3-methylaminoisothiazole S-oxide **2c** possesses an (*S*) absolute configuration.

2.3. Computational analysis of the oxidation mechanism

With the aim to better understand the reason for the observed enantioselectivities of the oxidation reactions herein reported, we performed DFT calculations in order to analyze the transition structures leading to (*R*)- and (*S*)-enantiomers. As shown above, best results in terms of selectivity were obtained for the 4-halosubstituted isothiazole compounds **1d** and **1e** (ee: 65%), while the 5-halosubstituted compounds **1g** and **1f** show scarce enantioselectivity (ee: 6% and 5%, respectively). For these reasons, the reactions of oxaziridine (+)-**6b** with 4-bromo-isothiazole **1e** and 5-bromoisothiazole **1f**, respectively, are chosen as the model systems. The model is further simplified by replacing the benzyl substituent with a computationally affordable CH_3 group, as the experimental evidences show that the substitution pattern of the exocyclic nitrogen plays a little role in the stereochemical outcome of the oxidation reaction. Accordingly, in the following discussion reactants and products will be referred as **M1e**–**1f** and **M2e**–**2f**, respectively. As reported in Section 4.1, calculations are performed at both the B3LYP/6-31G(d) and B3LYP/6-31G(d,p),S(3df) levels of theory and the following discussions are referred to the latter method. Both the *endo* and *exo* approaches of the isothiazoles to the oxaziridine (+)-**6b** were evaluated, but only the structures corresponding to the *exo* transition state actually converged. This result can be explained by taking into account the huge steric hindrance of the oxaziridine ethylene bridge. The obtained transition state geometries, depicted in Figure 5, are in line with the 'planar' transition state models for the oxygen transfer from an oxaziridine to a sulfoxide, ethylene or H_2S obtained at the HF/4-31G level by Bach et al.[14] However, concerning the herein described transition states, located at both the B3LYP/6-31G(d) and B3LYP/6-31G(d,p),S(3df) levels, some differences are observable for the oxygen transfer mechanism.

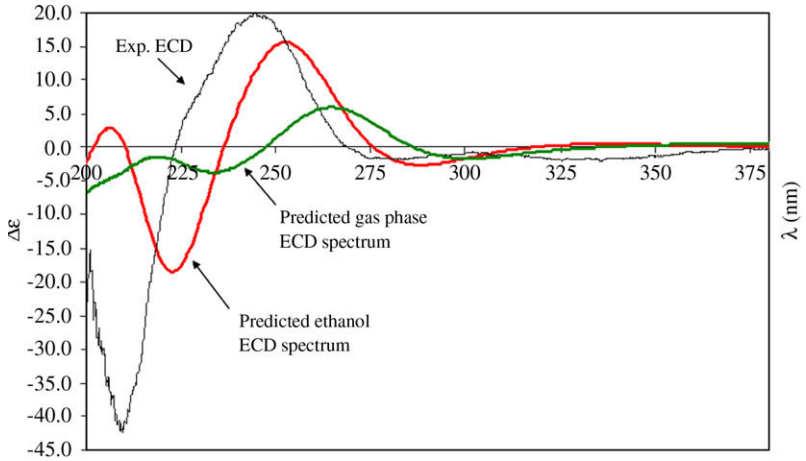

Figure 4. Experimental (black line) ECD spectrum of (+)-3-methylaminoisothiazole 1-oxide and predicted (TDDFT/B3LYP/aug-cc-pVDZ, velocity form) for (*S*)-3-methylisothiazole 1-oxide **2c** in gas phase (green line) and ethanol (red line).

Indeed, the analysis of geometrical parameters of the planar transition state described by Bach for the oxidation of H_2S is evidence that the C–O and N–O oxaziridine bond cleavage occurs in a quite synchronous manner, as C–O and N–O distances resulted in 2.003 and 1.988 Å, respectively. On the other hand, the bond length reported in Table 7 reveals unequivocally that the oxygen transfer occurs asynchronously, with an initial N–O and a subsequent C–O cleavage. This behaviour could be due either to the steric and electronic properties of our specific structures, or to the different chosen theoretical level, as it includes electron correlation and a more extended basis set, particularly important for sulfur-containing structures. Seeking for an answer to the above-mentioned question we optimized at the B3LYP/6-31G(d,p),S(3df) level the transition state model for the oxygen transfer from an unsubstituted oxaziridine to H_2S, starting from both the 'spiro' and the 'planar' orientations reported by Bach. Both structures converged to a unique geometry, represented in Figure 6, perfectly comparable with the other transition states herein located, with N–O and C–O distances of 2.116 and 1.608 Å, respectively. The analysis of the vibrational motion associated with the unique imaginary frequency further confirmed the observed asynchronicity of this oxidation reaction.

Coming back to the main objective of this computational study, we will provide a possible explanation for the different enantioselectivities observed within the oxidation of 4- and 5-halosubstituted isothiazoles.

The activation energies reported in Table 7 show that **TS-(proS)M2e** is favoured over **TS-(proR)M2e** by 2.3 kcal/mol, while a decidedly lower energy difference is computed between **TS-(proS)M2f** and **TS-(proR)M2f**, as the former is favoured by only 0.2 kcal/mol. We have initially found such results quite surprising, as we thought that **TS-(proR)M2e** should have been stabilized by an attractive interaction between the C5–H and the SO_2 moiety (see Fig. 6). Indeed, H···O and C5···O distances and C5–H–O angle (2.954, 3.668 Å and 123.9 deg, respectively) measured for **TS-(proR)M2e** are perfectly comparable with the weak hydrogen interaction parameters reported by the literature.[28a,b]

However, as one can see from both Table 7 and Figure 5, such a weak hydrogen bond causes the oxaziridine oxygen to approach the isothiazole sulfur in a decidedly distorted manner (C5–S–O and N2–S–O angles measure 88.8 and 114.4 deg, respectively) if it is compared to the 'ideal' transition state structure represented by the simplified model in Figure 6, thus provoking the observed energetic raise. On the other hand, the oxygen approach in **TS-(proS)M2e** is decidedly favoured by the geometrical point of view. This behaviour further confirms that weak hydrogen interactions in transition states are sometimes critical in determining the stereo/regiochemical outcome of chemical reactions, as already observed for Diels–Alder and hetero-Diels–Alder cycloadditions as well as other coupling reactions.[29,30] On the other hand, isothiazole **M2f**, being substituted at C-5 by an halogen atom, is not able to interact with the SO_2 moiety, thus the oxaziridine oxygen approaches the sulfur atom in a quite symmetric manner with respect to the isothiazole ring in both **TS-(proS)** and **TS-(proR)M2f**, thus explaining a similar computed energy. It should be noted that in **TS-(proR)M2f** the S–O forming bond is slightly distorted if com-

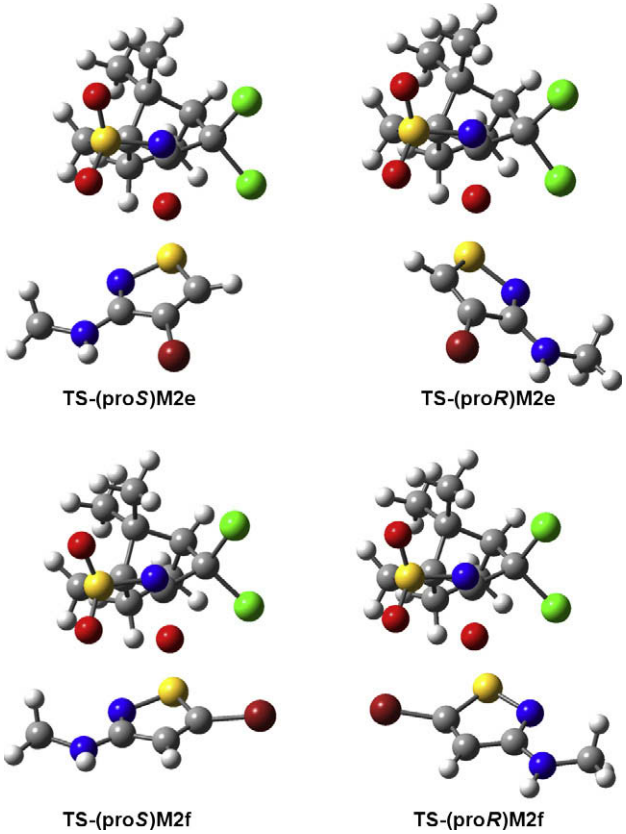

Figure 5. Transition states leading to (***S***)**-M2e**, (***R***)**-M2e**, (***S***)**-M2f** and (***R***)**-M2f**.

Table 7
Selected geometrical parameters (Å, deg) and imaginary frequencies (cm^{-1}) of located transition states, together with ZPE corrected activation energies (kcal/mol)[a]

Compd	S–O	C–O	N–O	C5–S–O	N2–S–O	IF	$\Delta E^{\ddagger}$
TS-(pro*S*)M2e	1.918	1.467	2.051	92.6	97.4	−359.54	22.7
TS-(pro*R*)M2e	1.931	1.496	2.043	88.8	114.4	−398.56	25.0
TS-(pro*S*)M2f	1.923	1.469	2.049	90.5	97.4	−371.47	22.7
TS-(pro*R*)M2f	1.944	1.477	2.045	91.2	104.5	−381.68	22.9

[a] Results from B3LYP/6-31G(d,p),S(3df) calculations are herein reported. The sum of isolated reactants' energies is taken as reference.

pared with the (**proS**) structure, which indeed is favoured in terms of relative energy, in perfect concordance with the observed experimental results.

3. Conclusion

In conclusion, we have described results of the oxidation of prochiral sulfur of 3-aminosubstituted isothiazoles affording new chiral 3-aminosubstituted isothiazole S-oxides by two different approaches consisting in the oxidation of (i) an achiral compound by way of an enantiopure oxaziridine which allowed to obtain the sulfoxide derivatives with good ee, (ii) an enantiopure compound which did not give interesting results in terms of diastereoselection but offered the possibility to isolate the two diastereomers through chromatographic separation and crystallization. Among the different oxaziridines tested, the reagent of choice is (+)-((8,8-dichlorocamphoryl)sulfonyl)oxaziridine (+)-**6b**, which is very efficient under microwave irradiation. To the best of our knowledge, the binomial camphorylsufonyloxaziridine-microwave irradiation has never been used in isothiazole oxidation until now. The influence on the stereochemical outcome of the reaction exerted by the substituents was also considered. We found that the presence of a halogen as substituent on C-4 of the heterocyclic ring increases the enantiomeric excess, which does not occur when the halogen is on C-5. The observed differences in terms of enantioselectivity are explained with the aid of theoretical calculations. Indeed, it is found that the formation of a weak hydrogen bond between the isothiazole H-5 and the oxygen of the camphorylsulfonyloxaziridine, observed only for the transition state leading to the (*R*)-4-halo-substituted isothiazole 1-oxide, destabilizes the transition state itself and thus the (*S*)-stereoisomer corresponds to experimental findings. Thus, a new interpretation of the oxidation reaction mechanism has been provided on the basis of B3LYP/6-31G(d,p),S(3df) calculations. The absolute configuration to the stereogenic sulfur atom was assigned by a comparison of the experimental optical activities and ECD measurements with those theoretically predicted at the TDDFT/B3LYP/aug-cc-pVDZ level of theory.

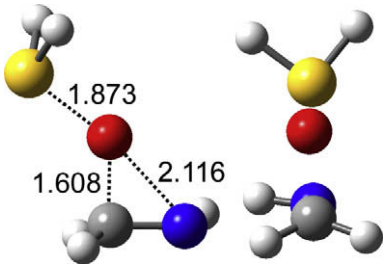

Figure 6. Orthogonal views of the simplified transition state model for the oxygen transfer, obtained at the B3LYP/6-31G(d,p),S(3df) level. Distances are reported in Å.

4. Experimental section

4.1. Theoretical calculations

Optical rotation analyses were carried out following the protocol described below. The starting geometries were generated by conformational analysis with the SPARTAN02 software,[31] using molecular mechanics (MMFF94s force field) and retaining all the structures differing by 2 kcal/mol in energy or less. All these geometries were fully optimized at the B3LYP/6-31G* level,[32,33] both in the gas phase and in the proper solvents. In all cases, the free energy values at $T = 298$ K were employed to calculate the population of each conformer, using the Boltzmann statistics. The geometry optimization of (*S*)-3-methylaminoisothiazole S-oxide conformers was repeated using the 6-31G** basis set and the energy difference of the two structures became 2.13 kcal/mol (vs 2.07 kcal/mole previously obtained using the 6-31G* basis set), thus obtaining populations of 97.3% and 2.7% (previously 97% and 3%). Such a small difference in population does not justify the use of the larger basis set. The calculations of the optical rotatory power were carried out at TDDFT/B3LYP/aug-cc-pVDZ level both in the gas phase and in solution.[34] The theoretical values of optical rotation (to be compared with the experimental ones) were obtained as weighted averages on the Boltzmann populations calculated in the gas phase or in the selected solvents. All the calculations of geometries, populations and optical rotatory power for solvated systems were obtained using a continuum solvation model, namely the Integral Equation Formalism version of the Polarizable Continuum Model (IEF-PCM).[26] In this framework, the solvent is represented as a polarizable continuum dielectric and the solute is assumed to be embedded in a molecular cavity of proper shape and dimension within such a dielectric. By introducing a proper surface charge distribution on the cavity surface representing the response of the solvent to the presence of the solute, it will be possible to quantify solvent induced changes both in the solute geometry and in its optical rotatory power.[24e] The ECD calculations were carried out following a known procedure.[35]

TS-(proS)M2e, **TS-(proR)M2e**, **TS-(proS)M2f** and **TS-(proR)M2f**, together with the corresponding reactants and products, were initially optimized in the gas phase using the B3LYP functional and the 6-31G* basis set. Vibrational frequencies were computed at the same level of theory in order to define optimized geometries as minima (no imaginary frequencies) or transition states (a unique imaginary frequency corresponding to the vibrational stretching of the forming/breaking bonds) and to calculate ZPVE and thermochemical corrections to electronic energies (1 atm, 298.15 K). It was reported that an adequate description of the geometry and electronic properties of sulfur-containing compounds would require the inclusion of supplementary d functions in the basis set,[36] thus all stationary points were reoptimized at the B3LYP/6-31G(d,p),S(3df) level and confirmed by a vibrational analysis at the same level of theory. Geometries and relative energies within the two theoretical levels were quite comparable: energy difference between **TS-(proS)** and **TS-(pro-**

R)**M2e** resulted −1.8 and −2.3 kcal/mol with the former and the latter more accurate method, respectively, while the relative energy between **TS-**(**pro*S***) and **TS-**(**pro*R***)**M2f** resulted −0.5 and −0.3 kcal/mol at the B3LYP/6-31G(d) and B3LYP/6-31G(d,p),S(3df) levels, respectively. All QM calculations were performed with the GAUSSIAN 03 package.[37]

^{1}H NMR spectra were obtained in the solvents indicated with 200 or 300 MHz instruments. Coupling constants (*J*) are given in hertz. Mass spectra were obtained by electron impact ionization at 70 eV using the direct exposure probe (DEP).

Compounds **1b**,**c**,**g**[16–18,38] **4**,[39] **5**,[10] and **6c**–**d**,[11] were prepared according to the procedure given in the literature. Compounds **6a**,**b** are commercially available.

4.2. Synthesis of 3-aminosubstituted isothiazoles

4.2.1. *N*-Benzyl-5-bromo-isothiazol-3-amine 1f

Compound **1b** (1.04 mmol) was dissolved in anhydrous THF (15 mL) and the solution cooled at −60 °C under nitrogen. Next, LDA (2.10 mL of a 2 M solution in THF) was added and after about 5–10 min. solid BrCN (2.08 mmol) was added and stirred. At the end of the reaction (TLC cyclohexane/ethyl acetate 3:1), the solvent was evaporated and the mixture was taken up with CH_2Cl_2 (30 mL) and washed with water (3 × 10 mL). The organic phase was dried with Na_2SO_4, filtered and evaporated to dryness affording an impure oil, which was purified by column chromatography (cyclohexane/ethyl acetate 100:0 to 0:100) affording pure **1f**. Yield: 51%, mp 97–98 °C (yellow powder from Et_2O/pentane). IR 3340 cm^{-1} (NH). ^{1}H NMR ($CDCl_3$): δ = 4.51 (s, 2H; CH_2), 4.74 (br s, 1H; NH), 6.46 (s, 1H; H-4), 7.26–7.36 (m, 5H; ArH) ^{13}C NMR ($CDCl_3$): δ = 47.7 (CH_2), 115.3 (C-4), 127.7, 127.8, 128.9 (ArCH), 134.9 (ArC), 139.0 (C-5), 165.1 (C-3). MS (EI) *m*/*z* = 269.4 (M+, 100). Anal. Calcd for $C_{10}H_9BrN_2S$ (269.06): C, 44.62; H, 3.37; N, 10.41. Found: C, 44.45; H, 3.54; N, 10.16.

4.3. General procedure for the preparation of isothiazolamines 1a,d,e

The opportune isothiazole 3-one[16] was dissolved in $POCl_3$ (3 mL for each gram of reagent) under stirring at room temperature. When the reagent was completely consumed (TLC ethyl acetate, about 2–24 h), the solvent was evaporated under reduced pressure. Diethylether was added to the mixture (2 × 5 mL) at 0 °C and a deep orange oil was separated. Decantation of the solvent afforded a gum perfectly suitable for the next step. This gum was suspended in CH_3CN (30 mL) and NH_3 gas was bubbled for about 1 h under stirring at 0 °C. The reaction mixture was brought to room temperature and the solvent was evaporated under reduced pressure. The residue was purified by column chromatography (AcOEt/cyclohexane 0:100 to 100:0).

4.3.1. *N*-Benzyl-4-chloro-isothiazol-3-amine 1d

Yield: 40%. Mp oil. IR 3418 cm^{-1} (NH). ^{1}H NMR ($CDCl_3$): δ = 4.65 (d, *J* = 4.4 Hz, 2H; CH_2), 5.07 (br s, 1H; NH), 7.26–7.40 (m, 5H; ArH), 8.24 (s, 1H; H-5). ^{13}C NMR ($CDCl_3$): δ = 47.8 (CH_2), 110.1 (C-4), 127.9, 128.2, 129.1 (ArCH), 139.1 (ArC), 141.9 (C-5), 160.5 (C-3). Anal. Calcd for $C_{10}H_9ClN_2S$ (224.61): C, 53.45; H, 4.04; N, 12.47. Found: C, 53.68; H, 4.14; N, 12.20.

4.3.2. *N*-Benzyl-4-bromo-isothiazol-3-amine 1e

Yield: 55%. Mp yellow oil. IR 3415 cm^{-1} (NH). ^{1}H NMR ($CDCl_3$): δ = 4.63 (d, *J* = 6.2 Hz, 2H; CH_2), 5.25 (br s, 1H; NH), 7.22–7.42 (m, 5H; ArH), 8.40 (s, 1H; H-5). ^{13}C NMR (CD_3COCD_3): δ = 46.9 (CH_2), 95.4 (C-4), 127.0, 127.7, 127.4 (ArCH), 140.3 (ArC), 145.5 (C-5), 161.9 (C-3). MS (EI) *m*/*z* = 269 (M+, 100). Anal. Calcd for $C_{10}H_9BrN_2S$ (269.06): C, 44.62; H, 3.37; N, 10.41. Found: C, 44.27; H, 3.10; N, 10.02.

4.3.3. (*S*)-3-(1-Phenylethyl)-isothiazol-amine 1a

Yield: 42%. Mp 127–128 °C (white powder from CH_2Cl_2/Et_2O). IR 3300 cm^{-1} (NH). ^{1}H NMR ($CDCl_3$): δ = 1.56 (d, *J* = 6.6 Hz, 3H; CH_3), 4.88 (m, 1H; CH), 4.93 (m, 1H; NH), 6.33 (d, *J* = 4.8 Hz, 1H; H-4), 7.20–7.41 (m, 5H; ArH), 8.31 (d, *J* = 4.8 Hz, 1H; H-5) ^{13}C NMR ($CDCl_3$): δ = 24.1 (CH_3), 53.8 (CH), 111.6 (C-4), 126.2, 127.3, 128.8 (ArCH), 145.0 (ArC), 147.7 (C-5), 165.5 (C-3). MS (EI) *m*/*z* = 205 (M+, 100). Anal. Calcd for $C_{11}H_{12}N_2S$ (204.29): C, 64.67; H, 5.92; N, 13.71. Found: C, 64. 89; H, 5.86; N 13.56.

4.3.4. Synthesis of 2a

Equimolecular amounts (0.56 mmol) of **1a** and **4** were dissolved under stirring in CH_2Cl_2 (20 mL) at room temperature and the progress of the reaction was checked by TLC (AcOEt; 12 h). The solvent was evaporated under reduced pressure at room temperature. The residue was chromatographed on silica gel (eluent: cyclohexane/AcOEt 100:0 to 0:100) affording the two diastereoisomers (*S*,*S*)-**2a** and (*R*,*S*)-**2a**. Total yields 80%.

4.4. General procedure for the oxidation of 1a,b,c.d,e,g with (+) and (−)-6a,b

Equimolecular amounts (0.24 mmol) of the opportune 3-aminoisothiazole and (+)- or (−)-**8a**,**b** were dissolved in CH_2Cl_2 (5 mL) and irradiated with microwaves (400 W, 80 °C) for the time indicated in Tables 3 and 4. The solvent was evaporated under reduced pressure and the residue was chromatographed on silica gel (eluent: cyclohexane/AcOEt 100:0 to 0:100) affording pure sulfoxides **2a**,**b**,**c**.**d**,**e**,**g**. Compounds (*S*,*S*)-**2a** and (*S*,*R*)-**2a** can be obtained with 98% purity (chiral HPLC analyses) after column chromatography and crystallization with H_2O/MeOH.

Yields, ee% and de % are reported in Tables 3 and 4.

4.4.1. 3-(*S*)-(1-Phenylethyl)aminoisothiazol-(*S*)-1-oxide (*S*,*S*)-2a[40]

Mp 149–151 °C dec (after recrystallization from MeOH/H_2O: 98% purity). ^{1}H NMR ($CDCl_3$): δ = 1.63 (d, *J* = 7 Hz, 3H; CH_3), 5.26 (m, 1H; CH), 6.39 (m, 1H; NH), 6.74 (d, *J* = 5.5 Hz, 1H; H-4), 7.26–7.37 (m, 5-H: ArH), 7.72 (d, *J* = 5.5, 1H; H-5) ^{13}C NMR ($CDCl_3$): δ = 22.09 (CH_3), 53.08 (CH), 126.63, 127.94, 129.01 (ArCH), 129.25 (C-4; CH), 142.32 (ArC), 155.92 (C-5; CH), 164.87 (C-3; Cq). MS (EI) *m*/*z* = 221 (M+, 100) Anal. Calcd for $C_{11}H_{12}N_2OS$ (220.07): C, 59.97; H, 5.49; N, 12.72. Found: C, 59. 75; H, 5.76; N, 12.46. $[\alpha]_D$ = −133.3 (*c* 1, $CHCl_3$ calculated on a sample with de 74.64%) HPLC 20 μL loop on Chiralcel ODH, (*iso*propanol/hexane 30:70), flow: 1 mL min^{-1}, retention time 8.89 min.

4.4.2. 3-(*S*)-1-Phenylethyl)aminoisothiazole-(*R*)-1-oxide (*S*,*R*)-2a

Mp 138–140 °C dec ^{1}H NMR ($CDCl_3$): δ = 1.58 (d, *J* = 7 Hz, 3H; CH_3), 5.24 (m, 1H; CH), 6.43 (t, 1H; NH), 6.70 (d, *J* = 5.1 Hz, 1H; H-4), 7.26–7.34 (m, 5-H: ArH), 7.62 (d, *J* = 5.1, 1H; H-5) ^{13}C NMR ($CDCl_3$): δ = 21.56 (CH_3), 53.07 (CH), 126.72, 128.13, 129.02 (ArCH), 128.70 (C-4; CH), 142.12 (ArC), 155.74 (C-5; CH), 164.38 (C-3; Cq). MS (EI) *m*/*z* = 219.2 (M+, 100). Anal. Calcd for $C_{11}H_{12}N_2OS$ (220.07): C, 59.97; H, 5.49; N, 12.72. Found: C, 60.19; H, 5.80; N, 12.40. $[\alpha]_D$ = −353.6 (*c* 1, $CHCl_3$, calculated on a sample with de 82.30%) HPLC 20 μL loop on on Chiralcel ODH, (*iso*propanol/hexane 30:70), flow: 1 mL min^{-1}, retention time 6.27 min.

4.4.3. *N*-Benzyl-isothiazol-3-amine S-oxide 2b

Mp 94 °C (powder from CH_2Cl_2/Et_2O). IR 3208 cm^{-1} (NH). ^{1}H NMR (CD_3COCD_3): δ = 4.70 (d, *J* = 5.9 Hz, 2H; CH_2), 7.04 (d,

J = 5.5 Hz, 1H; H-4), 7.30–7.47 (m, 5H; ArH), 7.94 (br s, 1H; NH), 8.02 (d, J = 5.5 Hz, 1H; H-5) ^{13}C NMR (CD_3COCD_3): δ = 45.6 (CH_2), 97.2 (C-4), 126.6–127.7 (ArCH), 137.1 (ArC), 157.0 (C-5), 164.2 (C-3). MS (EI) m/z = 207 (M+, 100). Anal. Calcd for $C_{10}H_{10}N_2OS$ (206.26): C, 58.25; H, 4.85; N, 13.59. Found: C, 56.29; H, 5.18; N, 12.96. $[\alpha]_D$ = +36.6 (c 1, $CHCl_3$, calculated on a sample with ee 39.72%); $[\alpha]_D$ = +50.6 (c 1, $CHCl_3$, calculated on a sample with ee 55%); HPLC separation of (*R*)- and (*S*)-**2a**: 20 μL loop on Chiralcel ODH, (*iso*propanol/hexane 30:70), flow: 1 mL min^{-1}, retention time (*R*)-**2a** 7.74 min; (*S*)-**2a** 10.78 min.

4.4.4. *N*-Methyl-isothiazol-3-amine S-oxide 2c

Mp 119 °C (powder from CH_2Cl_2/Et_2O). IR 3225 cm^{-1} (NH). ^{1}H NMR (CD_3OD): δ = 3.05 (s, 3H; CH_3), 6.96 (d, J = 5.3 Hz, 1H; H-4), 7.99 (d, J = 5.3 Hz, 1H; H-5) ^{13}C NMR (CD_3OD): δ = 28.7 (CH_3), 128.7 (C-4), 156.0 (C-5), 167.8 (C-3). MS (EI) m/z = 130 (M+, 100). Anal. Calcd for $C_4H_6N_2OS$ (130): C, 36.91; H, 4.65; N, 21.52. Found: C, 36.57; H, 4.78; N, 21.33. $[\alpha]_D$ = −60 (c 1, methanol), ee 43.6% and +69 (c 1, methanol), ee 49.6%. HPLC separation of (*R*)- and (*S*)-**2c**: 20 μL loop on Chiralcel OF, (*iso*propanol/hexane 35:65), flow: 1 mL min^{-1}, retention time (*R*)-**2c** 27.9 min; (*S*)-**2c** 36.6.

4.4.5. *N*-Benzyl-5-chloro-isothiazol-3-amine S-oxide 2g

Mp 127–129 °C (powder from CH_2Cl_2/Et_2O). IR 3053 cm^{-1} (NH). ^{1}H NMR ($CDCl_3$): δ = 4.50–4.74 (m, 2H; CH_2), 6.74 (s, 1H; H-4), 7.08 (bs, 1H; NH), 7.28–7.39 (m, 5H; ArCH) ^{13}C NMR ($CDCl_3$): δ = 46.8 (CH_2), 122.7 (C-4), 128.4, 129.1 (ArCH), 136.5 (ArC), 163.9, 165.5 (C-5, C-3). MS (EI) m/z = 240 (M+, 100). Anal. Calcd for $C_{10}H_9ClN_2OS$ (240.45): C, 49.90; H, 3.77; N, 11.64. Found: C, 49.73; H, 3.82; N, 11.31. $[\alpha]_D$ = −5 (c 1, $CHCl_3$) ee 5.53% HPLC separation of (*R*)- and (*S*)-**2g**: 20 μL loop on Chiralcel ODH, (*iso*propanol/hexane 30:70), flow: 1 mL min^{-1}, retention time (*R*)-**2g** 7.08 min; (*S*)-**2g** 9.72 min.

4.4.6. *N*-Benzyl-4-chloro-isothiazol-3-amine S-oxide 2d

Mp 143–144 °C (powder from CH_2Cl_2/Et_2O). IR 3247 cm^{-1} (NH). ^{1}H NMR (DMSO-d_6): δ = 4.50–4.55 (m, 2H; CH_2), 7.20–7.40 (5H; ArH), 8.52 (s, 1H; H-5), 9.02 (br s, 1H; NH) ^{13}C NMR (DMSO-d_6): δ = 46.7 (CH_2), 127.9, 128.2, 129.0 (ArCH), 131.0 (C-4), 138.4 (ArC), 152.3 (C-5), 160.9 (C-3) MS (EI) m/z = 241 (M+, 100). Anal. Calcd for $C_{10}H_9ClN_2OS$ (240.45): C, 49.90; H, 3.77; N, 11.64. Found: C, 50.23; H, 3.53; N, 11.31. HPLC separation of (*R*)- and (*S*)-**2d**: 20 μL loop on Chiralcel OD, (*iso*propanol/hexane 3:6), flow: 1 mL min^{-1}, retention time (*R*)-**2d** 10.9 min; (*S*)-**2d** 15.0.

4.4.7. *N*-Benzyl-5-bromo-isothiazol-3-amine S-oxide 2f

Mp 123–124 °C (powder from CH_2Cl_2/Et_2O). IR 3225 cm^{-1} (NH). ^{1}H NMR ($CDCl_3$): δ = 2.07 (br s, 1H; NH), 4.55–4.62 (m, 2H; CH_2), 6.89 (s, 1H; H-4), 7.19–7.32 (m, 5H; ArH) ^{13}C NMR ($CDCl_3$): δ = 46.8 (CH_2), 127.7 (C-4), 127.2, 128.3, 129.0 (ArCH), 136.4 (ArC), 151.3 (C-5), 166.4 (C-3). MS (EI) m/z = 285.3 (M+, 100). Anal. Calcd for $C_{10}H_9BrN_2SO$ (285.05): C, 42.12; H, 3.18; N, 9.82. Found: C, 41.94; H, 3.28; N, 9.68. $[\alpha]_D$ = +6.0 (c 1, $CHCl_3$) ee 6.4% HPLC separation of (*R*)- and (*S*)-**2f**: 20 μL loop on Chiralcell OD, (*iso*propanol/hexane 3:7), flow: 1 mL min^{-1}, retention time (*R*)-**2f** 6.92 min; (*S*)-**2f** 8.34 min.

4.4.8. *N*-Benzyl-4-bromo-isothiazol-3-amine S-oxide 2e

Mp 158 °C (after recrystallization from MeOH/H_2O: 98% purity). IR 3220 cm^{-1} (NH). ^{1}H NMR (CD_3COCD_3): δ = 4.73 (d, J = 5.1 Hz, 2H; CH_2), 7.30–7.48 (m, 5H; ArH), 7.98 (br s, 1H; NH), 8.40 (s, 1H; H-4). ^{13}C NMR (CD_3COCD_3): δ = 47.5 (CH_2), 120.1 (C-4), 128.2, 128.7, 129.5 (ArCH), 138.6 (ArC), 156.8 (C-5), 161.7 (C-3). MS (EI) m/z = 287 (M+). Anal. Calcd for $C_{10}H_9BrN_2SO$ (285.05): C, 42.12; H, 3.18; N, 9.82. Found: C, 42.34; H, 3.25; N, 9.57. $[\alpha]_D$ = +130.95 (c 1, $CHCl_3$, calculated on a sample with ee 55.76%); $[\alpha]_D$ = +152.6 (c 1, $CHCl_3$, calculated on a sample with ee 65%) HPLC separation of (*R*)- and (*S*)-**2e**: 20 μL loop on Chiralcel ODH, (*iso*propanol/hexane 30:70), flow: 1 mL min^{-1}, retention time (*R*)-**2e** 12.25 min; (*S*)-**2e** 15.64 min.

Acknowledgements

The authors thank the Ministero dell'Istruzione, dell'Università e della Ricerca (MIUR) for the financial support (First and PRIN) and the Centro Interuniversitario Lombardo per l'Elaborazione Automatica (CILEA) for providing computational facilities.

References

1. (a) Clerici, F.; Gelmi, M. L.; Pellegrino, S. Isothiazoles. In *Comprehensive in Heterocyclic Chemistry III*; Katritzky, A. R., Ramsden, C. A., Scriven, E. F. V., Eds.; Elsevier: Oxford, UK, 2008; Vol. 4, pp 545–633. Chapter 4.05; (b) Chapman, R. F.; Peart, B. J. Isothiazoles. In *Comprehensive in Heterocyclic Chemistry II*; Katritzky, A. R., Rees, C. W., Scriven, E. F. V., Eds.; Pergamon Press: Oxford, 1996; Vol. 3. Chapter 3.07; (c) Khalaj, A.; Adibpour, N.; Shahverdi, A. R.; Daneshtalab, M. *Eur. J. Med. Chem.* **2004**, *39*, 699–705; (d) Zani, F.; Vicini, P.; Incerti, M. *Eur. J. Med. Chem.* **2004**, *39*, 135–140; (e) Da Settimo, F.; Primofiore, G.; La Motta, C.; Sartini, S.; Taliani, S.; Simorini, F.; Marini, A. M.; La Vecchia, A.; Novellino, E.; Boldrini, E. *J. Med. Chem.* **2005**, *48*, 6897–6907.
2. Clerici, F.; Lo Presti, L.; Gelmi, M. L.; Soave, R. *Tetrahedron* **2002**, *58*, 5173–5178. and references cited therein.
3. Clerici, F.; Contini, A.; Corsini, A.; Ferri, N.; Grzesiak, S.; Pellegrino, S.; Sala, A.; Yokoyama, K. *Eur. J. Med. Chem.* **2006**, *41*, 675–682.
4. Clerici, F.; Gelmi, M. L.; Yokoyama, K.; Pocar, D.; Van Voorhis, W. C.; Buckner, F. S.; Gelb, M. H. *Bioorg. Med. Chem. Lett.* **2002**, *12*, 2217–2220.
5. Clerici, F.; Corsini, A.; Ferri, N.; Gelb, M. H.; Yokoyama, K.; Pocar, D. *Biochem. Pharmacol.* **2005**, *70*, 1735–1743.
6. Casoni, A.; Clerici, F.; Contini, A.; Pellegrino, S.; Sala, A. *Lett. Org. Chem.* **2008**, *5*, 623–627.
7. Pellissier, H. *Tetrahedron* **2007**, *63*, 1297–1330.
8. Waldner, A. *Tetrahedron Lett.* **1989**, *30*, 3061–3064.
9. Davis, F. A.; Sheppard, A. C. *Tetrahedron* **1989**, *45*, 5703–5742.
10. Davis, F. A.; Reddy, R. T.; Han, W.; Carrol, P. J. *J. Am. Chem. Soc.* **1992**, *114*, 1428–1437.
11. Davis, F. A.; Kumar, A.; Chen, B.-C. *J. Org. Chem.* **1991**, *56*, 1143–1145.
12. Davis, F. A.; Billmers, J. M.; Gosciniak, D. J.; Towson, J. C.; Bach, R. D. *J. Org. Chem.* **1986**, *51*, 4240–4245.
13. Davis, F. A.; Weismiller, M. C.; Murphy, C. K.; Reddy, R. T.; Chen, B.-C. *J. Org. Chem.* **1992**, *57*, 7274–7285.
14. Bach, R. D.; Wolber, G. *J. Am. Chem. Soc.* **1984**, *106*, 1410–1415.
15. Bach, R. D.; Coddens, B. A.; Mc Dovall, J. J.; Schlegel, H. B.; Davies, F. A. *J. Org. Chem.* **1990**, *55*, 3325–3330.
16. Bell, A. S.; Fishwick, C. W. G.; Reed, J. E. *Tetrahedron* **1999**, *55*, 12313–12330.
17. Lewis, S. N.; Miller, G. A.; Hausman, M.; Szamborski, E. C. *J. Heterocycl. Chem.* **1971**, *8*, 571–580.
18. Weiler, E. D.; Petigara, R. B.; Wolfersberger, M. H.; Miller, G. A. *J. Heterocycl. Chem.* **1977**, *14*, 627–630.
19. Bunch, L.; Krogsgaard-Larsen, P.; Madsen, U. *J. Org. Chem.* **2002**, *67*, 2375–2377.
20. Katritzky, A. R.; Laurenzo, K.; Relyea, D. *Can. J. Chem.* **1988**, *66*, 1617–1624.
21. (a) Polavarapu, P. L. *Mol. Phys.* **1997**, *91*, 551–554; (b) Polavarapu, P. L. *Tetrahedron: Asymmetry* **1997**, *8*, 3397–3401; (c) Polavarapu, P. L. *Chirality* **2002**, *14*, 768–781.
22. (a) Kondru, R. K.; Wipf, P.; Beratan, D. N. *J. Am. Chem. Soc.* **1998**, *120*, 2204–2205; (b) Kondru, R. K.; Lim, S.; Wipf, P.; Baratan, D. N. *Chirality* **1997**, *9*, 469–477.
23. (a) Pecul, M.; Ruud, K. *Adv. Quantum. Chem.* **2006**, *50*, 185–227; (b) Crawford, T. D. *Theor. Chem. Acc.* **2006**, *115*, 227–245.
24. Very recent examples of assignment of absolute configuration by the ab initio calculation of $[\alpha]_D$ and ECD spectra are: (a) Stephens, P. J.; McCann, D. M.; Butkus, E.; Stoncius, S.; Cheeseman, J. R.; Frisch, M. J. *J. Org. Chem.* **2004**, *69*, 1948–1958; (b) Stephens, P. J.; McCann, D. M.; Devlin, F. J.; Cheeseman, J. R.; Frisch, M. J. *J. Am. Chem. Soc.* **2004**, *126*, 7514–7521; (c) Sebert, S.; Konig, G. M.; Voloshina, E.; Raabe, G.; Fleischhauer, J. *Chirality* **2006**, *18*, 413–418; (d) Stephens, P. J.; Pan, J. J.; Devlin, F. J.; Cheesman, J. R. *J. Nat. Prod.* **2008**, *71*, 285–2888; (e) Mennucci, B.; Claps, M.; Evidente, A.; Rosini, C. *J. Org. Chem.* **2007**, *72*, 6680–6691; (f) Hussain, H.; Akhtar, N.; Draeger, S.; Schulz, B.; Pescitelli, G.; Salvadori, P.; Antus, S.; Kurtan, T.; Krohn, K. *Eur. J. Org. Chem.* **2009**, 749–756. and references cited therein.
25. (a) Stephens, P. J.; Devlin, F. J.; Cheeseman, J. R.; Frisch, M. J. *J. Phys. Chem. A* **2001**, *105*, 5356–5371; (b) Stephens, P. J.; McCann, D. M.; Cheeseman, J. R.; Frisch, M. J. *Chirality* **2005**, *17*, S52–S64. and references cited therein.
26. Tomasi, J.; Mennucci, B.; Cammi, R. *Chem. Rev.* **2005**, *105*, 2999–3093. and references cited therein.
27. Autschbach, J.; Jensen, L.; Schatz, G. C.; Electra Tse, Y. C.; Krykunov, M. *J. Phys. Chem. A* **2006**, *110*, 2461–2473.

28. (a) Desiraju, G. R. *Chem. Commun.* **2005**, 2995–3001; (b) Muthuraman, M.; Le Fur, Y.; Bagieu-Beucher, M.; Masse, R.; Nicoud, J. F.; Gorge, S.; Nangia, A.; Desiraju, G. R. *J. Solid State Chem.* **2000**, *152*, 221–228.
29. Nishio, M. *Tetrahedron* **2005**, *61*, 6923–6950.
30. (a) Contini, A.; Leone, S.; Menichetti, S.; Viglianisi, C.; Trimarco, P. *J. Org. Chem.* **2006**, *71*, 5507–5514; (b) Borsini, E.; Broggini, G.; Contini, A.; Zecchi, G. *Eur. J. Org. Chem.* **2008**, 2808–2816.
31. SPARTAN '02, *Wavefunction Inc.*, 18401 Von Karman Avenue, Suite 370, Irvine, CA 92612, 2002, http://www.wavefun.com/.
32. (a) Lee, C.; Yang, W.; Parr, R. G. *Phys. Rev. B* **1988**, *37*, 785–789; (b) Becke, A. D. *J. Chem. Phys.* **1993**, *98*, 5648–5652.
33. Frisch, M. J.; Pople, J. A.; Binkley, J. S. *J. Chem. Phys.* **1984**, *80*, 3265–3269.
34. Woon, D. E.; Dunning, T. H., Jr. *J. Chem. Phys.* **1993**, *98*, 1358–1371.
35. Giorgio, E.; Tanaka, K.; Ding, W.; Krishnamurty, G.; Pitts, K.; Ellestad, G. E.; Rosini, C.; Berova, N. *Bioorg. Med. Chem.* **2005**, *13*, 5072–5079.
36. (a) Roux, M. V.; Temprado, M.; Jimènez, P.; Dávalos, J. Z.; Notario, R.; Martín-Valcárel, G.; Garrido, L.; Guzmán-Mejía, R.; Juaristi, E. *J. Org. Chem.* **2004**, *69*, 5454–5459; (b) Juaristi, E.; Notario, R.; Roux, M. V. *Chem. Soc. Rev.* **2005**, *34*, 347–354; (c) Aversa, M. C.; Barattucci, A.; Bonaccorsi, P.; Contini, A. *J. Phys. Org. Chem.* **2009**. doi: 10.1002/poc.1557.
37. Frisch, M. J.; Trucks, G. W.; Schlegel, H. B.; Scuseria, G. E.; Robb, M. A.; Cheeseman, J. R.; Zakrzewski, V. G.; Montgomery, J. A., Jr.; Stratmann, R. E.; Burant, J. C.; Dapprich, S.; Millam, J. M.; Daniels, A. D.; Kudin, K. N.; Strain, M. C.; Farkas, O.; Tomasi, J.; Barone, V.; Cossi, M.; Cammi, R.; Mennucci, B.; Pomelli, C.; Adamo, C.; Clifford, S.; Ochterski, J.; Petersson, G. A.; Ayala, P. Y.; Cui, Q.; Morokuma, K.; Malick, D. K.; Rabuck, A. D.; Raghavachari, K.; Foresman, J. B.; Cioslowski, J.; Ortiz, J. V.; Stefanov, B. B.; Liu, G.; Liashenko, A.; Piskorz, P.; Komaromi, I.; Gomperts, R.; Martin, R. L.; Fox, D. J.; Keith, T.; Al-Laham, M. A.; Peng, C. Y.; Nanayakkara, A.; Gonzalez, C.; Challacombe, M.; Gill, P. M. W.; Johnson, B. G.; Chen, W.; Wong, M. W.; Andres, J. L.; Head-Gordon, M.; Replogle, E. S.; Pople, J. A. *GAUSSIAN 03*; Gaussian: Pittsburgh, PA, USA, 2003, http://www.gaussian.com/.
38. Clerici, F.; Contini, A.; Gelmi, M. L.; Pocar, D. *Tetrahedron* **2003**, *59*, 9399–9408.
39. Davis, F. A.; Stringer, O. D. *J. Org. Chem.* **1982**, *47*, 1174–1175.
40. Basing on our results we assumed that the major diastereoisomer obtained by using (+)-**6b** as the oxidant has an (*S*) configuration at the sulfur atom.